Nanoscale

Accepted Manuscript

This article can be cited before page numbers have been issued, to do this please use: Z. Pu, Z. Li, H. Wang, Y. Zhuo, R. Yuan and Y. Chai, *Nanoscale*, 2017, DOI: 10.1039/C6NR08631D.

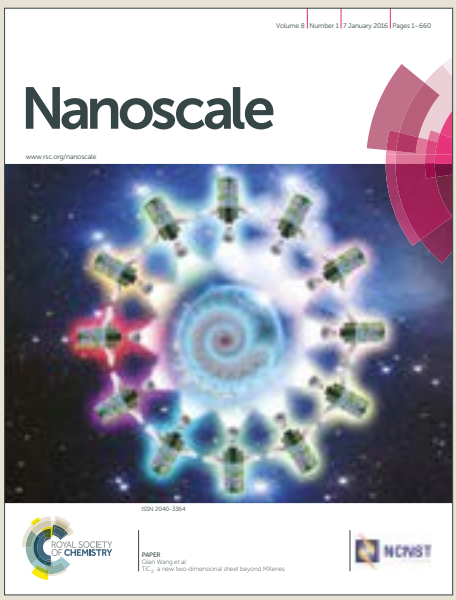

ROYAL SOCIETY OF CHEMISTRY

rsc.li/nanoscale

Cite this: DOI: 10.1039/c0xx00000x

www.rsc.org/xxxxxx

ARTICLE TYPE

DNA Nanomachine Based Regenerated Sensing Platform: a Novel Electrochemiluminescence Resonance Energy Transfer Strategy for Ultra-high Sensitive Detection of MicroRNA from Cancer Cells

Pu Zhang, Zhaoyang Li, Haijun Wang, Ying Zhuo, Ruo Yuan*, Yaqin Chai *

Received (in XXX, XXX) Xth XXXXXXXXX 20XX, Accepted Xth XXXXXXXXX 20XX
DOI: 10.1039/b000000x

The construction of DNA nanomachine holds great meanings in the development of DNA nanostructure, yet the real application of the nanomachine is still in its early stage. Furthermore, a one-step regenerated sensing platform for biomarkers detection in current researches remains a realistic challenge. Herein, a novel electrochemiluminescence resonance energy transfer (ERET) strategy between Alexa Flour 488 (AF 488) which is a kind of small molecule dye as the donor and CdSe@ZnS quantum dots (QDs) as the acceptor was reported, which was more easier to enter a cell and was applied for the construction of a DNA nanomachine-based regenerated biosensor for the ultra-high sensitive determination of cancer cells without any enzymes. First, a dual amplification strategy including target recycling and signal transformation was employed to achieve the conversion of a small number of miRNAs to a large amount of universal DNA reporters. Primordially, the DNA tweezer was kept in the "off" state with two arms labeling with QDs and AF488 respectively. Second, in the presence of the DNA reporters, the tweezer transformed to "on" state through the hybridization of reporter DNA and the exposed arms of the tweezer. Simultaneously, QDs and AF488 on the two arms were closed enough to generate ERET, increasing the ECL intensity of QDs remarkably. Impressively, the sensor could be regenerated by a one-step strand displacement and could be cycled for more than seven times. Owing to the dual amplification strategy and the high efficiency of the ERET between QDs and AF488, the proposed biosensor performed the linear range from 10 pM to 0.1 fM with a detection limit of 0.03 fM for miRNA determination, and the monitoring of different cancer cells was also achieved. Amazingly, the elaborated biosensor can also realize the sensitive detection of Pb^{2+}, which entailed the sensor be potentially used for field environmental analysis and monitoring, offering a new modular platform for the construction of functional DNA nanomachines in the ultra-high sensitive analysis of promising biomarkers and toxic metals.

Introduction

It is well known that cancer is one of the main causes of death among modern people. In particular, microRNA (miRNA) which is associated with tumor invasion, genomic instability, cell proliferation and immune responses plays a significant role in cancer research.[1,2] More recently, miRNA has been identified as a potential biomarker for diagnosis of cancer disease, clinical response and the prognosis.[3] Therefore, studying on the analysis of miRNAs is of significant importance in clinical medical diagnosis. Though considerable protocols for miRNA detection have gained attractive attentions and improvements, most of the methods cannot be regenerated,[4-6] which is the major problem of the sensing platform for miRNA analysis. The sensing platform must be reconstructed after it has been measured due to the inactivation of the biogenic segments and the breakage of the sensor during the determination.[7-9] Unfortunately, the reconstruction of the sensing architecture requires a few hours or even a few days, which makes the potential application of the biosensors costly and inconvenient. Therefore, constructing a regenerated sensing platform for miRNA analysis holds great meanings in early disease diagnostic applications with higher efficiency. While the current researches related to such aspect, especially in a one-step reaction to realize the regeneration, still remain a realistic challenge.

Various potential methods for miRNA detection were reported, including electrochemistry, photoelectrochemistry, chemiluminescence, fluorescence, electrochemiluminescence (ECL).[10-12] ECL is one of the most promising analysis methodologies to satisfy the needs of miRNAs detection owing to the high sensitivity, fast response, wide detection range, controllable reaction system and so on.[13, 14] Nowadays, with the development of ECL analytical protocol, ECL resonance energy transfer (ERET) has obtained increasing attention in detection of biomarkers because it can serve as the controllable and sensitive ECL switch for signal amplification.[15, 16] Nevertheless, the main challenge in improving the development of ERET is the difficulty in finding a pair of perfect energy overlapped donor/acceptor. For instance, Xu and her co-workers have researched an ERET strategy which selected CdS quantum dots (QDs) as the ECL donor and $Ru(bpy)_3^{2+}$ as the acceptor for developing a sensitive cytosensor.[17] Zhu and his co-workers have reported another QD-based ERET protocol which considered CdSe@ZnS QDs as the acceptor and luminol as the ECL donor for thrombin detection.[18] Recently, our previous work has reported a novel ERET system from $O_2/S_2O_8^{2-}$ to amino-terminated perylene derivative (PTC-

View Article Online
DOI: 10.1039/C6NR08631D

NH_2) for the detection of lead ion.[19] The current studies suggested that the high efficiency of ERET could enhance the ECL signal of emitter significantly. However, exploring suitable and attractive ECL donor/acceptor pairs are still limited by the lack of ECL regent with matched spectrum. Using a small molecule dye as the donor is especially important because the small molecule dye is more applicable for cell entry and staining which could be used to uncover the biological process of the cell with the dye-labeled biomarkers, while the study on the small molecule dye in ERET is rarely reported. Therefore, developing a new donor/acceptor pair of QD would highlight the potential significance of ERET in luminescence.

DNA, probably the most amazing molecule, is widely recognized as the central carrier of genetic information and it has gained comprehensive attention for the applications in nanotechnology.[20, 21] DNA based nanotechnology employs nucleic acid strands as the fundamental biological materials to construct the static nanostructures. Surprisingly, the nanostructures can present mechanical operations such as DNA machines, including "walkers", "spiders", "gears", "tweezers" and other nanomachines.[22] Among the synthetic DNA architectures, DNA tweezers consist of three or more DNA strands with tailored complementarity and the switching of the tweezer can be achieved with the help of a specific DNA sequence based on the strand hybridization of the two tails.[23] The studies on DNA tweezers performed the merits of motility, controllability and logicality, which lays the foundation of the bright future perspectives of the DNA tweezer in the progress of biosensing applications.

In the present work, an original ERET strategy from a fluorescence dye of Alexa Flour 488 (AF488) as an ECL donor to CdSe@ZnS quantum dots (QDs) as an ECL acceptor was studied for the first time. Based on the novel ERET system, we demonstrated a novel sensing platform that employed miRNA as the "fuel" to trigger the switching of the DNA tweezer on account of the dual amplification strategy including the target recycling and signal transformation, thus realizing the ultra-high sensitive analysis of miRNA. As shown in Scheme 1A, the dual amplification strategy was performed as follows. Firstly, target miRNA was introduced to open the hairpin DNA 1 (H1), obtaining a DNA duplex with an exposed end. With rationally design, the exposed end of the duplex was able to open another hairpin structure (H2). Next, the exposed end of the obtained DNA structure could open hairpin DNA 3 (H3), achieving a "Y" shaped structure with a specific sequences of Pb^{2+}-requiring DNAzyme and then releasing miRNA from the "Y" structure for another recycle. In the presence of Pb^{2+}, the recognition part of the DNAzyme was cleaved. With the shattering of "Y" structure, a large number of reporter DNA was produced to trigger the "on" state of the DNA tweezer. Simultaneously, as can be seen from Scheme 1B, a DNA tweezer was prepared by three kinds of DNA strands (A, B, and C). DNA strands B/C contained sequence 1 and sequence 2: sequence 1 was complementary with part of DNA strands A (purple part), sequence 2 was partially complementary with the reporter DNA (green part). DNA strand A was labeled with QDs and AF488 at the two ends of the strand. After that, the prepared DNA tweezer with an "off" state was incubated on the AuNPs modified sensing electrode surface through Au-S bond. Subsequently, the obtained reporter DNA was introduced on the sensor to "close" the tweezer by hybridizing with the exposure of strand B/C. Simultaneously, an enhancement of ECL signal from QDs was observed, because the proximity of CdSe@ZnS QDs and AF488 generated efficient ERET. Impressively, the proposed biosensor could be regenerated in 30 min after the incubation of an additional DNA S1 which was fully complementary with the green part of reporter DNA, switching the DNA tweezer into "off" state again. By measuring the ECL response of the CdSe@ZnS QDs, the proposed ECL biosensor for miRNA analysis suggested a wide linear range from 0.1 fM to 10 pM and a low detection limit of 0.03 fM with excellent stability and regenerability. Impressively, the sequences of B2/C2 could be replaced by other nucleic acid sequences including G-quadruplex, i-motifs or even DNAzymes, realizing various biomarkers or targets detection with the switching of the elaborated DNA nanotweezers. Inspired by the intellectual scientific interests, we intend to highlight that the subject of DNA nanomachine has promising future perspectives in the development of sensors by incorporating other leading edged technique.

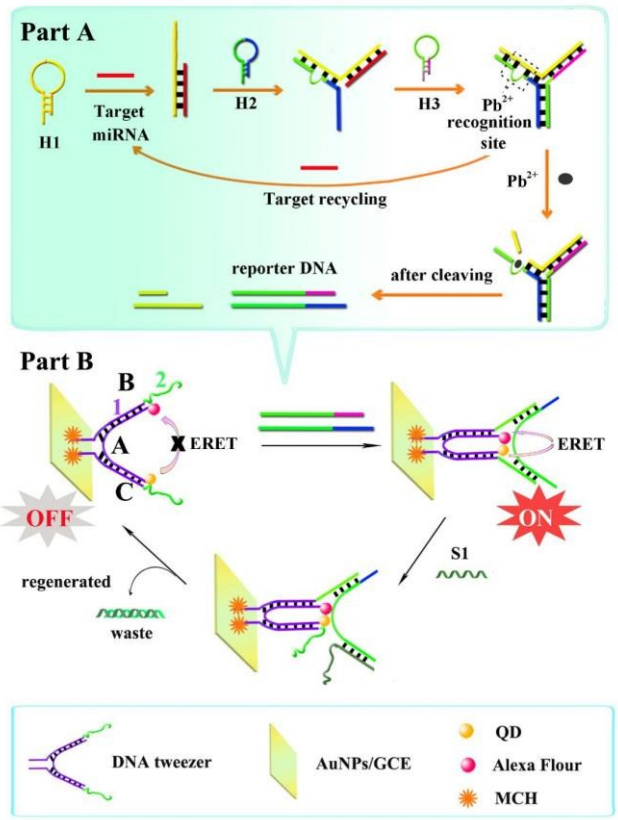

Scheme 1. Schematic description of the regenerated sensing DNA nanomachine based on a novel ERET system of QDs/AF488 for the ultra-sensitive determination of miRNA-21: the dual amplification strategy for the miRNA detection (Part A); the assembly of the DNA tweezer on the sensing electrode (Part B).

Experimental section

View Article Online
DOI: 10.1039/C6NR08631D

Reagents and apparatus

AF488 was purchased from Thermo Fisher Scientific (New York, USA). CdSe@ZnS QDs were provided by Jiayuan QDs Co. (Wuhan, China). $Pb(NO_3)_2$ and $K_2S_2O_8$ was got from Shanghai Chemical Reagent Co. (Shanghai, China). Tris (2-carbozyethyl) phosphine hydrochloride (TCEP), 6-mercaptohexanol (MCH), chlorauric acid ($HAuCl_4$), citrate sodium, N-(3-(Dimethylamino)propyl)-N′-ethylcarbodiimide hydrochloride (EDC), N-hydroxy succinimide (NHS), 3-(2-pyridyldithio) propionic acid N-hydroxysuccinimide ester (SPDP) and 1,4-dithiothreitol (DTT) was bought from Sigma-Aldrich (St. Louis, MO, U.S.A.). The buffer and detection solution used in this work were shown in ESI. Oligonucleotides applied in the paper were produced by Invitrogen Biotechnology Co., Ltd. (Shanghai, China) and the sequences are performed in Table S1 (See ESI). The analytical apparatus and measurements applied in this study were shown in ESI.

Preparation of AF488-A-CdSe@ZnS QDs

250 μL of AF488 (0.5 $mg \cdot L^{-1}$) was added into a mixture of EDC/NHS (4/1) and stirred for 15 min. 1 $\mu mol \cdot L^{-1}$ of DNA strand A was prepared with TAE/Mg^{2+} buffer and then mixed with the above AF488 solution for 2 h at room temperature (AF488-A). 6.2 mg of SPDP was dissolved in 1mL of DMSO with an ultimate concentration of 6.2 $mg \cdot mL^{-1}$. Afterwards, SPDP solution was mixed with CdSe@ZnS QDs uniformly. Then, the prepared AF488-A solution and DTT (diluted in acetic acid buffer with an ultimate concentration of 10 $mg \cdot mL^{-1}$) were reacted together for 2 h. The final AF488-A-CdSe@ZnS QDs solution was centrifuged and washed with PBS twice, then resuspended in 1 mL of PBS and kept at 4 ºC for further use.

Assembly of the miRNA biosensor

Different concentrations of miRNA-21 were incubated with H1 (0.5 μM), H2 (0.5 μM) and H3 (0.5 μM) for 3 h at 15 °C. Subsequently, Pb^{2+} (10 μM) was introduced in the above mixture for 0.5 h at 37 °C. The obtained solution was kept in the refrigerator for further use. The formation and cleaving of the "Y" structure were characterized by polyacrylamide gel electrophoresis (PAGE) in ESI.

Prior to assembly, bare GCE was polished using 0.3 and 0.05 μm alumina slurry to make the surface glow, followed by sonicating in the double distilled water, respectively. Then the sensing surface was immersed into $HAuCl_4$ (1%) and electrodeposited at 0.2 V with electrochemistry workstation for 30 s to obtain a gold nanoparticles (AuNPs) layer. After that, 10 μL of DNA A, B and C was modified on the electrode for 16 h, followed by incubating of MCH for 40 min on the electrode. The resulting sensor was assembled with 10 μL of AF488-A-CdSe@ZnS QDs solution for 2 h. Further, 15 μL of the prepared mixed solution of target, H1, H2, H3 and Pb^{2+} was dropping-coated on the sensor for 2 h to realize the analysis of target miRNA-21. At last, DNA S1 was incubated for 30 min to regenerate the sensor. The assembly of the DNA tweezer was characterized by PAGE in ESI.

Results and discussion

Investigation of ERET between CdSe@ZnS QDs and AF488

In order to study the ERET strategy, the ECL behavior of CdSe@ZnS QDs and AF488 was studied. As shown in Fig. 1A, the ECL emission peak of CdSe@ZnS QDs was observed at 633 nm by collecting the maximum ECL response during the cyclic potential sweep with a series of optical filters, the emission peak corresponding to AF488 was located at 520 nm (Fig. 1B). The ECL spectra of AF488-DNA strand A-CdSe@ZnS QDs was also studied, as demonstrated in Fig 1C, a dual ECL emission peak from the composite was observed, a low signal corresponding to AF488 and a strong signal corresponding to CdSe@ZnS QDs. This indicates that ERET between CdSe@ZnS QDs and AF488, namely energy transfer from the higher-band gap AF488 to the lower-band gap CdSe@ZnS QDs, was highly efficient. In order to further demonstrate the ERET between CdSe@ZnS QDs and AF488, the UV-vis absorption spectra of the acceptor (QDs) and the ECL emission spectra of donor (AF488) was carried out with the cyclic potential scanning from -2.0 to 0 V. As depicted in Fig. 2A, the UV-vis absorption spectra of CdSe@ZnS QDs (curve a) overlapped with the ECL emission spectra of the AF488 (curve b), suggesting the possibility of ERET between QDs and AF488. To further verify the ERET between CdSe@ZnS QDs and AF488, the ECL signal of CdSe@ZnS QDs with different concentrations of AF488 was investigated (Fig. 2B). With the increasing concentration of AF488, the ECL signal of CdSe@ZnS QDs increased significantly as expected. With the above experimental data, it could be assumed that the ERET would occur between CdSe@ZnS QDs and AF488, where AF488 emitted short wavelength as the ECL energy donor and CdSe@ZnS QDs emitted long wavelength as the ECL energy acceptor. The fluorescence responses were studied in the supporting information to further suggest the mechanism of the proposed ERET system (See Fig. S1 in ESI).

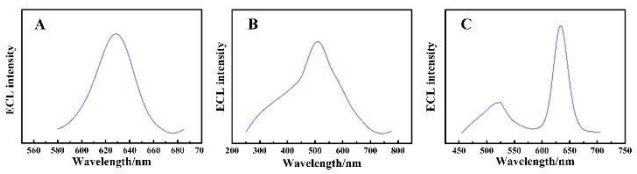

Fig. 1 The ECL spectra of (A) CdSe@ZnS QDs; (B) AF488; (C) the composite of AF488-DNA strand A-CdSe@ZnS QDs.

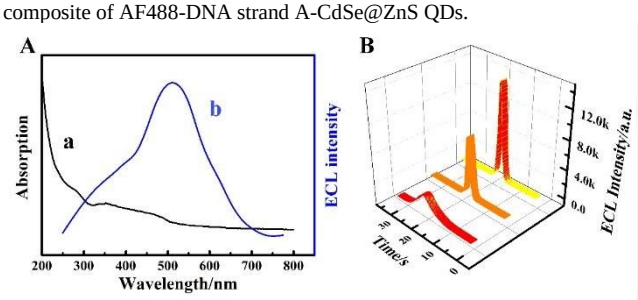

Fig. 2 (A) UV-vis absorption spectra of CdSe@ZnS QDs and ECL spectra of AF 488. (B) The ECL intensity of CdSe@ZnS QDs with different concentration of AF 488 (0.05 mg/ mL for curve a, 0.1 mg/mL for curve b, 0.5 mg/mL for curve c).

The electrochemical performance of the prepared sensor

The electrochemical performance of the elaborated sensor was investigated by CV and the result was depicted in Fig. 3A. The redox current of the AuNPs-electrodeposited GCE (curve b) showed an enhancement compared with bare GCE (curve a),

View Article Online
DOI: 10.1039/C6NR08631D

demonstrating the successful modification of AuNPs on the sensing surface. After the incubation of the assembled DNA tweezer, the CV current decreased which may owing to the semiconducting property of QDs and electron obstruction of DNA (curve c). The CV current of the sensor decreased after blocking with MCH (curve d), because MCH could hinder the electron transfer greatly. After that, the mixture of target, H1, H2, H3 and Pb^{2+} was incubated on the electrode, and the CV current decreased due to the electron hindrance of DNA molecules (curve e).

The ECL characterization of the elaborated biosensor

To represent the stepwise incubation procedure of the miRNA biosensor, ECL response of each modification step was recorded as depicted in Fig. 3B. After the DNA tweezer was assembled onto the electrode, an ECL response was observed due to the introduction of the ECL emitter (QDs) (curve a) and the DNA tweezer presented "off" state at that time. Subsequently, the ECL signal decreased after modifying with MCH due to the electron obstruction of MCH (curve b). Finally, when the sensing surface was incubated with target (10 pM), H1, H2, H3 and Pb^{2+}, the ECL signal increased significantly because the distance of AF488 and CdSe@ZnS QDs were closed, triggering the efficient energy transfer between AF488 and CdSe@ZnS QDs.

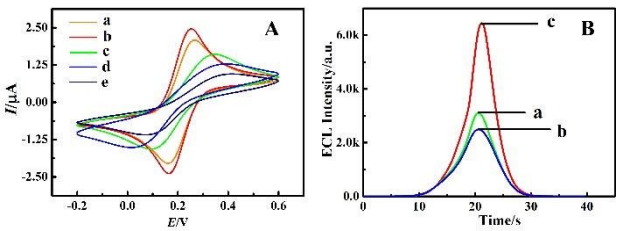

Fig. 3 (A) CVs of the modified steps detected in 5 mM $[Fe(CN)_6]^{3/4}$ solution: bare electrode (a), AuNPs/bare electrode (b), DNA tweezer/AuNPs/bare electrode (c), MCH/DNA tweezers/AuNPs/bare electrode (d), miRNA-21 mixed solution /MCH/DNA tweezers/AuNPs/bare electrode (e). (B) ECL response of the immobilization process was recorded in 0.05 M $S_2O_8^{2-}$ solution: DNA tweezers/AuNPs/bare electrode (a), MCH/DNA tweezer/AuNPs/bare electrode (b), miRNA-21 mixed solution/MCH/DNA tweezers/AuNPs/bare electrode (c).

The optimal condition of the analysis

To advance the performance of the designed biosensor, we have optimized the significant experimental conditions. In the present study, the quantity of the A/B/C DNA probes was a remarkable element affecting the analytical performance of biosensor. Thus, we have optimized the concentration of the above DNA chains with 10 pM of target. As depicted in Fig. 4A, in the presence of 0.05 M $S_2O_8^{2-}$, the ECL response increased with the reaction concentration up to 1 μM and remained constant after 1 μM. Thus, 1 μM of the A/B/C DNA probes were chosen for the analysis of miRNA-21.

The concentration of Pb^{2+} was another considerable parameter toward expected signal gains and was investigated as performed in Fig. 4B. The ECL signal increased along with the increasing of the Pb^{2+} concentration with 10 pM of target in the presence of 0.05 M $S_2O_8^{2-}$. When the concentration of Pb^{2+} was 10 μM, a plateau emerged and we chose 10 μM as the optimal concentration of Pb^{2+} in this study.

Besides, the optimal incubation time of Pb^{2+} was 30 min and the details were shown in ESI (Fig. S2).

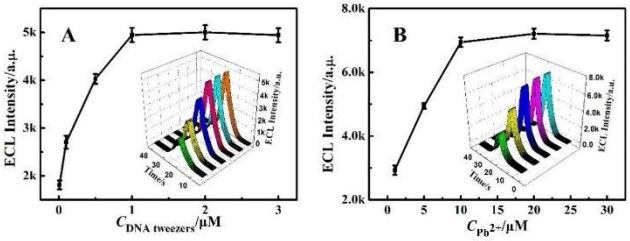

Fig. 4 Optimization of the analytical factors: (A) immobilized concentration of A/B/C DNA probes in the proposed sensor. (B) Incubated concentration of Pb^{2+} in the proposed biosensor.

ECL determination of the proposed biosensor for the detection of miRNA-21

Under the optimal conditions, the ECL intensity of CdSe/ZnS QDs increased with incremental concentration of miRNA. As can be figured out in Fig. 5, the calibration plot demonstrated an excellent linear relationship between logarithm of the miRNA-21 concentration and ECL signal in the range from 10 pM to 0.1 fM with a correlation coefficient of 0.9947. The regression equation for miRNA-21 is $I = 5876.08 + 1254.98 \lg c$, where c is the concentration of miRNA, and I is the ECL intensity obtained in this work. The detection limit is 0.03 fM according to the definition of LOD=$3S_b/m$ (where S_b is the standard deviation of the blank intensity and m is the slope of the calibration. As shown in Table 1, the performance of the biosensor for miRNA-21 is comparable and even better than the previous studies.

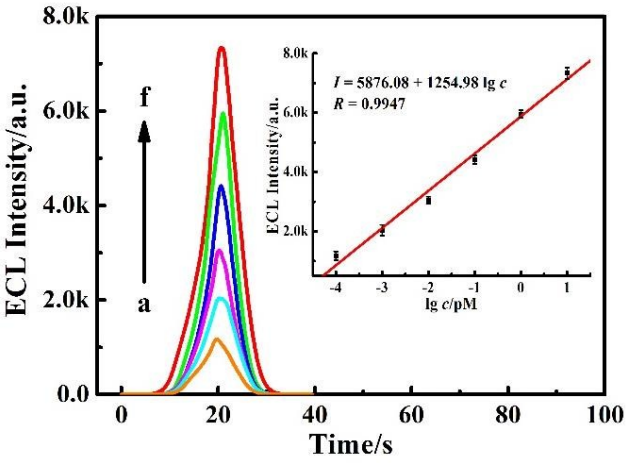

Fig. 5 ECL response of the proposed biosensor incubated with different concentrations of miRNA-21 and the calibration plots of ECL signal versus the logarithm of the miRNA concentration: (a) 10 pM, (b) 1, (c) 0.1 pM, (d) 0.01pM, (e) 1 fM, (f) 0.1 fM.

Table 1. The comparison of the elaborated biosensor with other analytical strategy.

View Article Online
DOI: 10.1039/C6NR08631D

method	target	detection limit	references
fluorescent	miRNA	1 fM	24
fluorescent	miRNA	10 fM	25
fluorescent	miRNA	1 pM	26
ECL	miRNA	10 fM	27
ECL	miRNA	0.5 fM	28
Colorimetric	miRNA	2 nM	29
ECL	miRNA	0.03 fM	This work

Interference studies

The specificity of the biosensor is an essential performance for miRNA-21 analysis. Therefore, we have assessed the specificity of our method with other non-target miRNAs (miRNA-141, miRNA-155 and the single-base mismatched miRNA). As can be seen in Fig. 6, the presence of miRNA-141 (100 pM), miRNA-155 (100 pM) and the single-base mismatched miRNA (100 pM) caused an insignificant increase in ECL intensity which agreed with that of the blank one. However, the ECL intensity corresponding to the target miRNA-21 at a lower (10-fold, 10 pM) concentration and the mixture containing miRNA-21 (10 pM) showed a significant ECL intensity, suggesting that the proposed biosensor has an outstanding selectivity for the discrimination between the target and non-target miRNA.

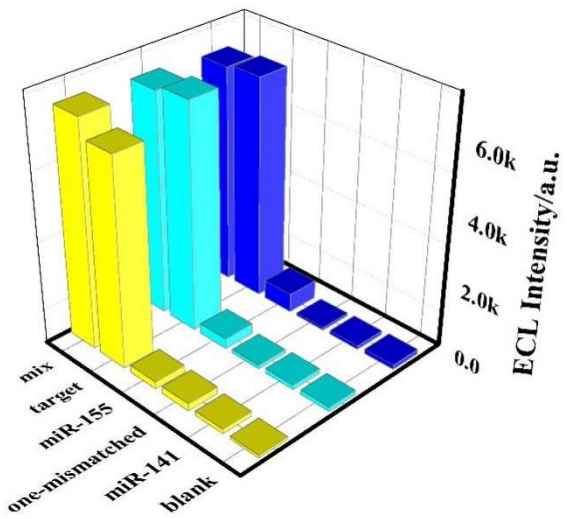

Fig. 6 The ECL response of three batches for miRNA-21 (10 pM) against the blank, miRNA-141 (100 pM), miRNA-155 (100 pM), the single-base mismatched miRNA (100 pM) and the mixture containing miRNA-21 of 10 pM.

Stability and reproducibility

The stability of the modified biosensor was studied for the analysis of 10 pM, 1 pM, 0.01 pM and 0.001 pM miRNA at the optimal analytical conditions. The result was showed in Fig. 7A, the stability investigation was performed by continuous scanning for 3 cycles and the result indicated the excellent stability of this biosensor. The result in Fig. 7B showed that the relative standard deviation (RSD%) for four successive assays was 4.07%. Moreover, the repeatability of the biosensor was investigated using four different modified electrodes for analysis and the result showed a RSD of 3.69%. As a consequence, the proposed biosensor endowed a remarkable stability and reproducibility.

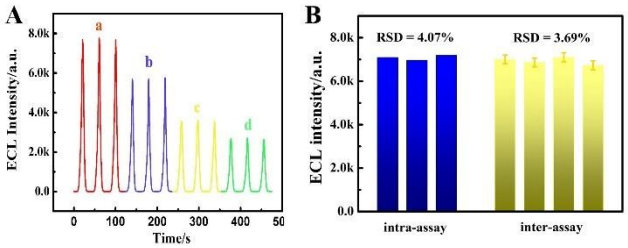

Fig. 7 (A) Stability of the prepared biosensor with miRNA-21 at the concentration of 10 pM (a), 1 pM (b), 0.01 pM (c) and 0.001 pM (d). (B) Reproducibility of the proposed biosensor.

Regenerability

To regenerate the biosensor, DNA S1 was introduced to fully hybridize with the reporter DNA, thus releasing the reporter from the DNA tweezer system and realizing the regeneration of the biosensor with one simple step. As can be depicted in Fig. 8A, compared with the original "off" state (curve a), the ECL signal increased significantly after hybridizing with the reporter DNA (curve b). After the incubation of DNA S1, the sensor regenerated with a suppressed ECL signal of 99.1% (curve c). Furthermore, the proposed biosensor could be reproduced over seven cycles for the analysis of miRNA-21 target (Fig. 8B). This result demonstrated that the proposed biosensor possessed desirable regenerability, representing another outstanding advantage of the sensing nanostructure.

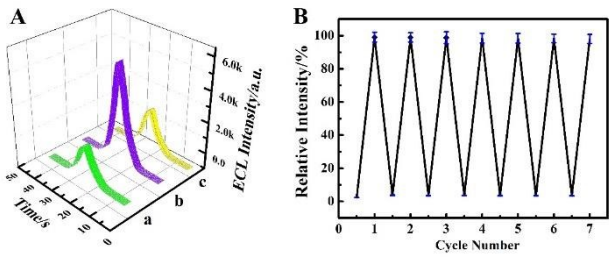

Fig. 8 (A) ECL intensity of the regenerated biosensor: the "off" state of the sensor (curve a), "on" state of the sensor (curve b), regeneration of the sensor with the representing of "off" state (curve c). (B) The ECL response for miRNA detection over seven cycles. The top dots represented the ECL signal of "on" state, whereas the bottom dots represented the ECL signal of "off" state.

Real application of the sensor in cancer cells

For investigating the capacity of the elaborated biosensor, Hela cancer cells and human breast (MCF-7) cancer cells was selected to carry out the ECL detection of miRNA-21 expression. After cell counting, the real samples for the practical application were obtained with a commercial miRNA extraction instrument. As shown in Fig. 9, the total RNAs from the cancer cells suggested a significant expression of MCF-7 and the ECL response increased with the increasing of cell numbers. While the blank and Hela ones depicted a relatively low expression comparing to MCF-7. The result obtained in this study was in accordance with the previous researches and represented that the DNA nanomachine-

View Article Online
DOI: 10.1039/C6NR08631D

based sensor endowed remarkable potential for further application in early cancer diagnostics and biomedical study.[30]

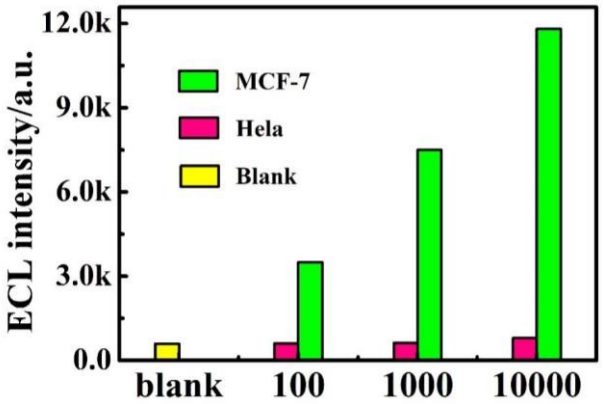

Fig. 9 The data analysis of the proposed biosensor from blank experiment, Hela and MCF-7 cancer cells with different cell numbers.

Conclusions

In summary, the present work demonstrated a novel ERET system between AF 488 as the donor and CdSe@ZnS QDs as the acceptor and its application of a DNA nanomachine-based sensing platform for the ultra-high sensitive detection of miRNA biomarkers. This study has brought forth the following three novel ideas. First, a new ERET system (AF 488/CdSe@ZnS QDs) is reported for the first time, which provides a new pair of ECL donor/acceptor which is more applicable for cell entry and staining to uncover the biological process of the cell with the dye-labeled biomarkers, broadening the promising application of ERET for various targets analysis. Second, the sensing platform realized the regeneration in a one-step displacement reaction, excusing the expensive and tedious reconstruction process of the formal sensing system. Third, the designed dual amplification strategy not only realized the target recycling, but also realized the conversion of a small quantity of miRNAs to a large amount of universal DNA reporters to activate the switching of the DNA nanomachines, achieving ultra-high sensitive analysis of miRNA-21 with the detection limit of 0.03 fM in cancer cells. Interestingly, the enzyme-free biosensor can also be employed to the sensitive detection of Pb^{2+} with the constant concentration of miRNA. With the ingenious combination of DNA nanomachines, the proposed biosensor exhibited excellent selectivity, accuracy and stability and provided a modular sensing platform for various target analysis, which may hold great significance in biosensing, early disease diagnose and environmental analysis.

Acknowledgements

This paper was financially supported by the National Natural Science Foundation of China (51473136, 21575116 and 21675129), the Fundamental Research Funds for the Central Universities (XDJK2016E055), China and China Postdoctoral Science Foundation (2016M602626).

Notes and references

Key Laboratory of Luminescent and Real-Time Analytical Chemistry (Southwest University), Ministry of Education, College of Chemistry and Chemical Engineering, Southwest University, Chongqing 400715, People's Republic of China

Tel: +86-023-68252277; Fax: +86-23-68253172

E-mail address: yuanruo@swu.edu.cn, yqchai@swu.edu.cn

1 G. A. Calin, C. M. Croce, *Nat Rev Cancer*, 2006, **6**, 857-866.

2 D. P. Bartel, *Cell*, 2009, **136**, 215-233.

3 A. Rodriguez, S. Griffiths-Jones, J. L. Ashurst, A. Bradley, *Genome Res*, 2004, **14**, 1902-1910.

4 C. Y. Xiong, H. J. Wang, W. B. Liang, Y. L. Yuan, R. Yuan and Y. Q. Chai, *Chem. Eur. J.*, 2015, **21**, 9825-9832.

5 P. Zhang, X.Y Wu, R. Yuan and Y. Q. Chai, *Anal. Chem.*, 2015, **87**, 3202-3207.

6 W. B. Liang, C. C. Fan, Y. Zhuo, Y. N. Zheng, C. Y. Xiong, Y. Q. Chai and R. Yuan, *Anal. Chem.*, 2016, **88**, 4940-4948.

7 X. B. Zhang, C. H. Liu, L. B. Sun, X. R. Duana and Z. P. Li, *Chem. Sci.*, 2015, **6**, 6213-6218.

8 L. D. Wang, R. J. Deng and J. H. Li, *Chem. Sci.*, 2015, **6**, 6777-6782.

9 P. Zhang, Y. Zhuo, Y. Y. Chang, R. Yuan and Y. Q. Chai, *Anal. Chem.*, 2015, **87**, 10385-10391.

10 P. Wu, X. D. Hou, J. J. Xu and H. Y. Chen, *Nanoscale*, 2016, **8**, 8427-8442.

11 S, Bi, M, Chen, X. Q. Jia and Y. Dong, *Nanoscale*, 2015, **7**, 3745-3753.

12 J. T. D. Bonis-O'Donnell, D. Vong, S. Pennathura and D. K. Fygenson, *Nanoscale*, 2016, **8**, 14489-14496.

13 L. Wu, J. S. Wang, L. Y. Feng, J. S. Ren, W. L. Wei and X. G. Qu, *Adv. Mater.*, 2012, **24**, 2447-2452.

14 M. Edwards, P. McConnell, D. A. Schafer and J. A. Cooper, *Nat. Commun.*, 2015, **6**, 8415

15 Y. Cheng, J. P. Lei, Y. L. Chen and H. X. Ju, *Biosence Bioelectron.*, 2014, **15**, 431-436.

16 N. Hao, X. L. Li, H. R. Zhan, J. J. Xu and H, Y, Chen, *Chem. Commun.*, 2014, **50**, 14828-14830.

17 Wu, M. S., Shi, H. W., Xu, J. J. and Chen, H. Y., *Chem. Commun.*, 2011, **47**, 7752-7754.

18 Y. P. Dong, T. T. Gao, Y. Zhou and J. J. Zhu, *Anal. Chem.*, 2014, **86**, 11373-11379.

19 A. Samanta and I. L. Medintz, *Nanoscale*, 2016, **8,** 9037-9095.

20 X. L. Shi, X. Y. Wu, T. Song and X. Li, *Nanoscale*, 2016, **8**, 14785-14792.

21 M. K. Beissenhirtz and I, Willner, *Org. Biomol. Chem.*, 2006, **4**, 3392-3401.

22 B. K. Mu 1ller, A. Reuter, F. C. Simmel and D. C. Lamb, *Nano Lett.*, 2006, **6**, 2814-2820.

23 B. C. Yin, Y. Q. Liu and B. C. Ye, *Anal. Chem.*, 2013, **85**, 11487-11493.

24 R. X. Duan, X. L. Zuo, S. T. Wang, X. Y. Quan, D. L. Chen, Z. F. Chen, L. Jiang, C. H. Fan and F. Xia, *J. Am. Chem. Soc.*, 2013, **135**, 4604-4607.

View Article Online
DOI: 10.1039/C6NR08631D

25 F. Z. Xu, H. Shi, X. X. He, K. M. Wang, D. G. He, Q. P. Guo, Z. H. Qing, L. A. Yan, X. S. Ye, D. Li and J. L. Tang, *Anal. Chem.*, 2014, **86**, 6976-6982.

26 Q. M. Feng, Y. Z. Shen, M. X. Li, Z. L. Zhang, W. Zhao, J. J. Xu, H. Y. Chen, *Anal. Chem.*, 2016, *88*, 937-944.

27 Y. H. Liao, R. Huang, Z. K. Ma, Y. X. Wu, X. M. Zhou and D. Xing, *Anal. Chem.*, 2014, **86**, 4596-4604.

28 T. Tian, H. Xiao, Z. G. Zhang, Y. L. Long, S. Peng, S. R. Wang, X. Zhou, S. M. Liu and X. Zhou, *Chem. Eur. J.*, 2013, **19**, 92-95.

29 Z. Y. Wan, J. X. Han, Y. Z. Cui, X. Y. Zhou and K. X. Fan, *Biochem. Biph. Res. Co.*, 2013, **439**, 384-389.